Photon production in heavy-ion collisions at SPS energies

G.Q. Li and G.E. Brown
Department of Physics, State University of New York at Stony Brook,
Stony Brook, NY 11793, USA

Single photon spectra in heavy-ion collisions at SPS energies are studied in the relativistic transport model that incorporates self-consistently the change of hadron masses in dense matter. We separate the total photon spectrum into 'background' arising from the radiative decays of π^0 and η mesons, and the 'themal' one from other sources. For the latter we include contributions from radiative decays of ρ, ω, η', and a_1, radiative decays of baryon resonances, as well as two-body processes such as $\pi\pi \to \rho\gamma$ and $\pi\rho \to \pi\gamma$. It is found that more than 95% of all photons come from the decays of π^0 and η mesons, while the thermal photons account for less than 5% of the total photon yield. The thermal photon spectra in our calculations with either free or in-medium meson masses do not exceed the upper bound set by the experimental measurment of the WA80 Collaboration.

pacs: 12.38.Mh, 24.10.Lx, 25.75.-q
Key words: single photon spectra, relativistic heavy-ion collisions, quark gluon plasma.

I. INTRODUCTION

One of the primary motivations of ultra-relativistic heavy-ion collisons is to create and study in the laboratory the properties of quark gluon plasma (QGP) as predicted by quantum chromodynamics (QCD). Experiments have been carried out at BNL-AGS and CERN-SPS energies, and will be continued at higher energies of BNL-RHIC and CERN-LHC colliders [1]. The measurement of electromagnetic observables such as photon and dilepton spectra constitutes a major part of these efforts. The main reason for this is that the photons and dileptons do not suffer strong final-state interactions as hadrons do. They can thus be considered as 'penetrating probes' of the initial hot and dense stages where the QGP might be formed in these ultra-relativistic heavy-ion collisions [2–5].

So far, the measurement of eletromagnetic observables has chiefly been carried out at CERN-SPS energies. Recent observation of the enhancement of low-mass dileptons in central heavy-ion collisions by the CERES [6–10] and Helios-3 collaborations [11] has generated a great deal of interest in the heavy-ion community. Different dynamical models, such as hydrodynamical and transport models, have been used to investigate this phenomenon [12–25]. Calculations based on 'conventional sources' such as Dalitz decay and direct vector meson decay that account for the dilepton spectra in proton-induced reactions fail to explain the observed enhancement in heavy-ion collisions. Various medium effects, such as the dropping vector meson masses [12–16,23,25] as first proposed by Brown and Rho [26], the modification of rho meson spectral function [18,19,27,28], and the enhanced production of η and/or η' [29,30], have been proposed to explain this enhancement.

Another piece of experimental data from CERN-SPS that have been discussed extensively is the single photon spectra in central S+Au collisions from the WA80 collaboration [33]. In this experiment, π^0 and η spectra were measured simultaneously, so that their contributions to single photon spectra can be subtracted. It was found that the direct photon excess over these background sources is about 5% for central S+Au collisions [31–33]. Similar measurement of inclusive photon spectra has been carried out by the CERES collaboration [34]. The results are very much in agreement with those of WA80, namely, the inclusive photon spectra can be basically explained by hadronic decay, particularly radiative decay of π^0 and η mesons.

Many hydrodynamical calculations have been carried out to study photon spectra in these reactions [35–41]. In all these calculations, it is found that the contributions from the QGP, if it were formed at all in these reactions, to the single photon yield is negligibly small. The major contributions to these so-called 'thermal' photons, namely, excessive photons over the background of π^0 and η radiative decays, come from hadronic interactions.

In a number of papers [36,38,41], the absence of significant thermal photons has been interpreted as an evidence for the formation of quark gluon plasma. Without phase transition, the initial temperature of the hadronic gas was found to be about 400 MeV [36,41]. This led to a large amount of thermal photons from hadronic interaction which was not observed experimentally. Including the phase transition, the initial temperature can be lowered to about 200 MeV [36,41], because of increased degrees of freedom. This lower initial temperature natually reduces the thermal photon yield to be in agreement with the WA80 data. There is, however, a major caveat in this type of analysis and reasoning, namely, the initial temperature in the hadronic scenarios depends sensitively on how many hadron resonances are included in the analysis. Indeed, in Ref. [24], it was found that including a reasonable amount of

hadron resonances the initial temperature can be reduced to about 250 MeV. Furthermore it was shown in Ref. [40] that, if all the hadron resonances with masses below 2.5 GeV are included, the initial temperature can be lowered to about 200 MeV. In both papers, it was shown that the WA80 photon data can be explained without invoking the formation of quark gluon plasma.

There are, up till now, no detailed transport model calculations for photon spectra in heavy-ion collisions at CERN-SPS energies. In Ref. [42], results from the Hadron-String dynamics (HSD), that includes photons from the decay of η', ω and a_1, were compared with the data and were found to be far below the upper bound set by the WA80 collaboration. However, photons can also be produced from the decay of rho mesons, baryon resonances, and two-body scattering processes such as $\pi\pi \to \rho\gamma$ and $\pi\rho \to \pi\gamma$, which were neglected in Ref. [42]. Whether the inclusion of these additional sources will bring the theoretical results close or even beyond the upper bound of the WA80 data needs to be studied.

One of the purposes of this paper is thus to calculate the single photon spectra in central S+Au collisions based on the relativistic transport model and to compare with hydrodynamical results. The other purpose is to see whether the same model that explains the enhancement of low-mass dileptons, as shown in Refs. [12–14], can also explain the lack of signal in the direct photon measurement. Explaining simultaneously these two correlated facts constitutes an important test for the consistency of the model.

This paper is arranged as follows: In Section 2 we recall briefly the main ingredients of the relativistic transport model. In Section 3 we discuss various source for photon production, inlcuding meson and baryon decay, as well as two-body scattering. We shall discuss radiative decay widths and photon production cross sections in two-body processes. The results are discussions are presented in Section 4. The paper ends with a brief summary in section 5.

II. THE RELATIVISTIC TRANSPORT MODEL AND HADRONIC OBSERVABLES

In studying medium effects in heavy-ion collisions, the relativistic transport model [43–45] based on the Walecka-type model [46] has been quite useful, as it provides a thermodynamically consistent description of the medium effects through the scalar and vector fields. In heavy-ion collisions at CERN-SPS energies, many hadrons are produced in the initial nucleon-nucleon interactions. This is usually modeled by the fragmentation of strings, which are the chromoelectric flux-tubes excited from the interacting quarks. One successful model for taking into account this nonequilibrium dynamics is the RQMD model [47]. To extend the relativistic transport model to heavy-ion collisions at these energies, we have used as initial conditions the hadron abundance and distributions obtained from the string fragmentation in RQMD.

Further interactions and decays of these 'primary' hadrons are then taken into account as in usual relativistic transport model. We include non-strange baryons with masses below 1.72 GeV, as well as Λ, Σ, $\Lambda(1405)$ and $\Sigma(1385)$. For mesons we include π, η, ρ, ω, η', a_1, and ϕ, as well as K and $K^*(892)$. Baryons are propagated in their mean fields, which are assumed to be the same for all non-strange baryons. The mean fields for hyperons are assumed to be 2/3 of that for non-strange baryons, based on the simple quark counting rule. Medium effects on pions and phi mesons are neglected, while those on kaons are always included, with their mean fields taken to be 1/3 of these for nucleons. For other non-strange mesons, we consider two scenarios as in Refs. [12–14], namely, one with medium effects and one without medium effects. In our model, these mesons are treated in the constituent quark model. They thus feel only the scalar potential that shifts their masses, since the vector potential on the (constiutent) quark is canceled by that on the (constituent) antiquark.

In addition to propagation in mean fields, hadrons also under stochastic two-body collisions. For baryon-baryon interactions, we include both elastic and inelastic scattering for nucleons, $\Delta(1232)$, $N(1440)$ and $N(1535)$. Their cross sections are either taken from Refs. [48,49] or obtained using the detailed balance procedure [50]. The meson-baryon interactions are modeled by baryon resonace formation and decay. For example, the interaction of a pion with a nucleon proceeds through the formation and decay of $\Delta(1232)$, $N(1440)$, ..., N(1720). The formation cross sections are taken to be of the relativistic Breit-Wigner form. The meson-meson interactions are either formulated by the resonance formation and decay when the intermediate meson is explicitly included in our model or treated as a direct elastic scattering with a cross section estimated from various theoretical models. Of particular importance for photon production are the pion-pion and pion-rho collisions, which are dominated by rho and a_1 meson formation, respectively.

As mentioned in the Introduction, the observed enhancement of low-mass dileptons in heavy-ion collisions can be explained by including dropping vector meson masses. It is useful to see whether the inclusion of the dropping vector meson mass is also consistent with the real photon data from the WA80 collaboration. For this purpose we will also calculate photon spectra in the scenario of dropping meson masses. Following Ref. [12–14], we extend the Walecka model from the coupling of nucleons to scalar and vector fields to the coupling of light quarks to these fields, using

the ideas of the meson-quark coupling model [52]. For a system of nucleons, pseudoscalar mesons, vector mesons, and axial-vector mesons at temperature T and baryon density ρ_B, the scalar field $\langle\sigma\rangle$ is determined self-consistently from

$$\begin{aligned} m_\sigma^2\langle\sigma\rangle &= \frac{4g_\sigma}{(2\pi)^3}\int d\mathbf{k}\frac{m_N^*}{E_N^*}\Big[\frac{1}{\exp((E_N^*-\mu_B)/T)+1}+\frac{1}{\exp((E_N^*+\mu_B)/T)+1}\Big] \\ &+ \frac{0.45g_\sigma}{(2\pi)^3}\int d\mathbf{k}\frac{m_\eta^*}{E_\eta^*}\frac{1}{\exp(E_\eta^*/T)-1}+\frac{6g_\sigma}{(2\pi)^3}\int d\mathbf{k}\frac{m_\rho^*}{E_\rho^*}\frac{1}{\exp(E_\rho^*/T)-1} \\ &+ \frac{2g_\sigma}{(2\pi)^3}\int d\mathbf{k}\frac{m_\omega^*}{E_\omega^*}\frac{1}{\exp(E_\omega^*/T)-1}+\frac{6\sqrt{2}g_\sigma}{(2\pi)^3}\int d\mathbf{k}\frac{m_{a_1}^*}{E_{a_1}^*}\frac{1}{\exp(E_{a_1}^*/T)-1}, \end{aligned} \tag{1}$$

where we have used the constituent quark model relations for the nucleon and vector meson masses [52], i.e., $m_N^* = m_N - g_\sigma\langle\sigma\rangle$, $m_{\rho,\omega}^* \approx m_{\rho,\omega} - (2/3)g_\sigma\langle\sigma\rangle$, the quark structure of the η meson in free space which leads to $m_\eta^* \approx m_\eta - 0.45g_\sigma\langle\sigma\rangle$, and the Weinberg sum rule relation between the rho-meson and a_1 meson masses, i.e, $m_{a_1}^* \approx m_{a_1} - (2\sqrt{2}/3)g_\sigma\langle\sigma\rangle$. Recently we found that the use of a refined model, the effective chiral Lagrangian of [53], leads to essentially the same results for dilepton spectra [54].

This model describes the hadron observables quite well. In Fig. 1 we show the pseudorapidity distribtion of charged particles (upper window) and transverse momentum spectra of pions (lower window) for central S+Au collisions. They are found to be in good agreement with the experimental data from the WA80 [55,56] and the CERES collaboration [57]. Comparisons with other hadron observables, such as proton rapidity distribution and transverse mass spectra can be found in Ref. [14].

III. PHOTON PRODUCTION: RADIATIVE WIDTHS AND CROSS SECTIONS

The majority of single photons come from the decay of π^0 and η mesons at freeze out. The background photon spectra from their decay can thus be evaluated at the end of the transport model simulation by using the following branching ratio [58]

$$B_{\pi^0\to\gamma\gamma} = \frac{\Gamma_{\pi^0\to\gamma\gamma}}{\Gamma_\pi^0} = 0.988, \quad B_{\eta\to\gamma\gamma} = \frac{\Gamma_{\eta\to\gamma\gamma}}{\Gamma_\eta} = 0.3925. \tag{2}$$

For the 'thermal' photon spectra we include the decay of ρ, ω, η', and a_1 mesons, the decay of all the baryon resonances in our model, as well as two-body processes such as $\pi\pi \to \rho\gamma$ and $\pi\rho \to \pi\gamma$. The decay widths for $\rho^0 \to \pi^+\pi^-\gamma$ and $\rho^\pm \to \pi^\pm\pi^0\gamma$ are taken from [59], which explains the measured width for $\rho^0 \to \pi^+\pi^-\gamma$. The mass dependence of these widths are shown in Fig. 2. The open circle gives the experimental data for $\rho^0 \to \pi^+\pi^-\gamma$ [58]. Note that in transport models, rho mesons can have different masses because of its broad mass distribution, so mass dependent widths are used.

The omega meson radiative decay width $\Gamma_{\omega\to\pi^0\gamma}$ was studied in Ref. [60] based on the chiral Lagrangian that includes the Wess-Zumino anomalous term. The width was found to be proportional to the pion momentum in the ω rest frame, namely,

$$\Gamma_{\omega\to\pi^0\gamma}(M) = C|\mathbf{p}_\pi|^3 \approx 0.01316|\mathbf{p}_\pi|^3, \tag{3}$$

where $|\mathbf{p}_\pi| = (M^2 - m_\pi^2)/(2M)$ and the coefficient C is determined from the measured width [58].

There exists only one experimental measurement of the a_1 radiative decay width, using the reverse process of a_1 production in pion-nucleus collisions [61]. The width is found to be $\Gamma_{a_1\to\pi\gamma} = 0.64 \pm 0.246$, which was used in Ref. [42] in calculating a_1 contribution to photon production. In Ref. [62], an effective Lagrangian was proposed to calculate this width, which turns out to be about 1.4 MeV using the vector dominance assumption. This is close to the prediction of non-relativistic quark model of about 1.0-1.6 MeV [63]. In view of large uncertainties, we use $\Gamma_{a_1\to\pi\gamma}(m_{a_1}) = 1$ MeV as in Refs. [13,14]. According to Ref. [62], in the limit that pion momentum is much greater than its mass, the a_1 radiative decay width is given by

$$\Gamma_{a_1\to\pi\gamma}(M) = C|\mathbf{p}_\pi|^5 \approx 0.01214|\mathbf{p}_\pi|^5, \tag{4}$$

where the coefficient C is determined by using $\Gamma_{a_1\to\pi\gamma}(m_{a_1}) = 1$ MeV.

Photons can also be produced from the decay of baryon resonaces. These contributions are usually neglected in hydrodynamical calculations [36,41]. The radiative decay widths for baryon resonances included in our transport

model have been measured experimentally through photon-nucleon and/or pion-nucleon interactions [58]. We use these widths in our calculation of their contributions to single photon spectra. In addition, Σ^0 decay dominantly into $\Lambda\gamma$. But since the mass difference between Σ^0 and Λ is not very large, photons from Σ^0 decay usually have low transverse momenta, as will be shown below.

For contributions from two-body processes, we include $\pi\pi \rightarrow \rho\gamma$ and $\pi\rho \rightarrow \pi\gamma$, which are the most important ones in the temperature region relevant for SPS energies [64,65]. These cross sections were first evaluated in Ref. [64], with an effective Lagragian including π, η, ρ, and ω mesons, which will be used in the present work. The cross section for $\pi\pi \rightarrow \rho\gamma$ is shown in Fig. 4, for three different rho meson masses. As the rho meson mass is reduced, the threshold and also the magnitude of the cross section are reduced. The cross section for $\pi\rho \rightarrow \pi\gamma$ is shown in Fig. 5 for three different rho meson mass. When the rho meson mass is reduced, the available center-of-mass energy is reduced and the cross section increases.

The importance of the a_1 meson was investigated in Refs. [62,65]. Since in our transport model the processes $\pi\rho \rightarrow a_1$ and $a_1 \rightarrow \pi\gamma$ are explictly included, we need not to include the effects of a_1 on the direct $\pi\rho \rightarrow \pi\gamma$ process. Otherwise there will be double counting. The effects of the a_1 on $\pi\pi \rightarrow \rho\gamma$ were found to be appreciable for photons with energies greater than about 0.5 GeV [65]. The contributions of $\pi\pi \rightarrow \rho\gamma$ to these 'hard' photons are, however, extremely small (about one to two orders of magnitude smaller than those from $\pi\rho \rightarrow \pi\gamma$). This justifies our use of the cross sections given in Ref. [64] that did not include the a_1 meson in the model.

IV. PHOTON PRODUCTION: RESULTS AND DISCUSSIONS

We present in this section the single photon spectra in central S+Au collisions at 200 AGeV. The acceptance of the WA80 collaboration is taken into account, namely, we include photons with pseudo-rapidity of $2.1 < \eta < 2.9$. In Fig. 6 we show the background photon spectra from the decay of π^0 (dotted line) and η meson (dashed line). It is seen that contribution from π^0 decay far dominates the background.

The contributions to the so-called 'thermal' photons from the decay of mesons and baryons, and from two-body scattering are shown in Fig. 7. The ω radiative decay is found to be the most important source for photons with transverse momenta above about 0.5 GeV. This is in agreement with the finding of Ref. [42], although our results are somewhat larger than those of Ref. [42]. This difference might be traced back to the difference in the 'primary' ω meson abundances in the RQMD and the HSD models. The contribution from the a_1 radiative decay is comparable to that from direct $\pi\rho \rightarrow \pi\gamma$. This is in agreement with the conclusion of Ref. [65] that including a_1 the $\pi\rho$ contribution increases by about a factor 2-3 in the relevant temperature and photon energy region.

The contributions from η' and Σ^0 radiative decays are restricted to photons with transverse momenta below 0.5 GeV, because the mass differences between hadrons in the intial and final states in these processes are small. Photons with transverse momenta below 0.2 GeV come chiefly from the decay of Σ^0 and $\pi\pi$ scattering. The reaction $\pi\pi \rightarrow \rho\gamma$ is endothermic, with most of the available energy going into the rho meson mass. This cross section actually diverges as the photon energy goes to zero. We have included a low-energy cut-off as in Ref. [64]. The choice of this cut-off parameter affects basically only the photons with transverse momenta below about 0.1 GeV, where no experimental data are available.

In Fig. 8 we compare our results with the upper bound of the WA80 collaboration. More than 80% of thermal photons come from meson decay, of which more than half come from the ω radiative decay. Overall, our results are well below the WA80 upper bound for photons with transverse momenta below 1 GeV. For higher tranverse momenta, our results touch the upper bound of the experimental data. Our results are actually very close to those of Ref. [24] with the parameter set named EOS H, that includes about the same number of hadron degrees of freedom as in our model. The conclusion is thus that the WA80 single photon data do not necessary imply the formation quark gluon plasma. Of course, the possibility of quark gluon plasma formation is not ruled out.

Next we discuss the results obtained with in-medium meson masses. The separate contributions from the decay of mesons and baryons, and two-body processes are shown in Fig. 9. There is not much change in the meson and baryon decay contributions. With dropping meson masses, the abundances of ρ and a_1 mesons increase [13,14]. This is, however, compensated by the decreases in their radiative decay widths (see Figs. 2 and 3). The comparison of total thermal photon spectra with the experimental data is given in Fig. 10. In the case of dropping meson masses, our results do not exceed the upper bound of the WA80 data.

Finally, in Fig. 11 we show the ratio of total (sum of thermal and background) photon to the background photon. In both and free meson mass and in-medium meson mass cases, the thermal photon accounts for less than 5% of all the single photons, in agreement with the experimental observation, and the simple estimation by Tserruya in Ref. [8]. An important difference between dilepton and real photon measurements is that in the former case, the contamination from $\pi^0 \rightarrow \gamma e^+e^-$ can, in principle, be removed since these dileptons are restricted to masses below m_{π^0}, while in the

real photon case, the $\pi^0 \to \gamma\gamma$ contributes to photons with any momentum. The subtraction of the background, and hence the measurement of interesting signals, are much more subtle in the real photon case [8].

V. PHOTON PRODUCTION: COMPARISON WITH OTHER CALCULATIONS

The WA80 single photon data have been looked at by several groups, mostly based on hydrodynamical models [22–24,35–39,41,42] Here we compare our results that are based on the relativistic transport model with some of these results. In Fig. 12, we show our results together with those from [24] and [36]. In Ref. [24] different equations of state with and without quark gluon plasma formation were considered. Shown in the figure by dotted line is their results based on EOS H. This equation of state included about the same number of hadron degrees of freedom as in our transport model. It is very interesting to see that their results are very similar to ours, although the dynamical models used are quite different. In Ref. [36] two different equations of state, one with quark gluon plasma formation and one with pure pionic gas, were considered. Shown in the figure is their results based on the pionic gas equation of state. Because of very limited number of hadronic degrees of freedom in this equation of state, they needed a very high initial temperature to account for the final observed hadron abundances. This led to large photon yield.

In Refs. [21,22]. Steele *et al.* studied photon as well as dilepton production at SPS energy based on the master equation formalism. They have considered two scenarios, one with pions only and the other includes nucleon as well. In order to make a fair comparison, we show in the upper window of Fig. 13 the photon spectra obtained in our calculation with the decays of ρ and a_1 and two-body processes of $\pi\pi \to \rho\gamma$ and $\pi\rho \to \pi\gamma$, and the results of Ref. [22] excluding nucleons. We can see that their results are very similar to ours. In the lower part of Fig. 13 we compare our results including baryon resonance decay with those of Ref. [22] that included nucleon effects. The results are again quite consistent with ours. Note that the results of Ref. [22] is very sensitive to the initial nucleon density. The results shown in the lower part of Fig. 13 were obtained with an initial nucleon density $\rho_N = 0.7\rho_0$, which is quite appropriate for S+Au collisions at SPS energies.

VI. SUMMARY

In summary, we studied single photon spectra in central S+Au collisions at SPS energies using the relativistic transport model that has been used to study dilepton spectra in the same reactions. We included photons from the background sources of π^0 and η decays, as well as thermal sources such as meson decays, decays of baryon resonances, and two-body processes. We found that more than 95% of single photons come from the decays of π^0 and η. The thermal photons account for only less than 5% of all single photons, in agreement with the experimental observation made by the WA80 and CERES collaborations. We compared our thermal photon spectra with the experimental upper bound extracted by the WA80 collaboration. It is seen that in both the free meson mass and in-medium meson mass cases, our results do not exceed the experimental upper bound. This indicates that our model can explain both the enhancement of low-mass dileptons and the lack of signal in the real photon measurement. Our results are also in agreement with the conclusions of hydrodynamical calculations of Refs. [24,40] that included a sufficient number of hadron degrees of freedom. Therefore the WA80 single photon data do not necessary imply the phase transition to the quark gluon plasma, as claimed in Refs. [36,38,41] based on a limited number of hadron degrees of freedom.

Finally, we note that the elementary radiative decay widths and photon prodcution cross sections used in this study have been taken from different models. In principle, most of them can be evaluated consistently within the same model, such as the hidden gauge theory of [66]. In this model, one can also study the effects of the change of gauge coupling constant on photon production in hot and dense matter. Work in this direction is in progress and will be reported elsewhere [67].

We thank M.A. Halasz, C.M. Ko, J.V. Steele and I. Zahed for discussions, and I. Tserruya for a careful reading of the manuscript and useful suggestions. This work is supported in part by the Department of Energy under grant No. De-FG-88ER40388.

[1] See e.g., QM'95, Nucl. Phys. A590 (1995); QM'96, Nucl. Phys. A610 (1996).
[2] E.V. Shuryak, Phys. Lett. B79 (1978) 135.
[3] L.D. McLerran and T. Toimela, Phys. Rev. D 31 (1985) 545.
[4] K. Kajantie, J. Kapusta, L. McLerran, and A. Mekjian, Phys. Rev. D 34 (1986) 2746.
[5] R.V. Ruuskanen, Nucl. Phys. A544 (1992) 169c.
[6] G. Agakichiev *et al.*, Phys. Rev. Lett. 75 (1995) 1272.
[7] J. P. Wurm for the CERES Collaboration, Nucl. Phys. A590, 103c (1995).
[8] I. Tserruya, Nucl. Phys. A590 (1995) 127c.
[9] G. Agakichiev *et al.,* Nucl. Phys. A610 (1996) 317c.
[10] A. Drees, Nucl. Phys. A610 (1996) 536c.
[11] M. Masera for the HELIOS-3 Collaboration, Nucl. Phys. A590 (1995) 93c.
[12] G. Q. Li, C. M. Ko, and G. E. Brown, Phys. Rev. Lett. 75 (1995) 4007.
[13] G. Q. Li, C. M. Ko, and G. E. Brown, Nucl. Phys. A606 (1996) 568.
[14] G. Q. Li, C. M. Ko, G. E. Brown, and H. Sorge, Nucl. Phys. A611 (1996) 539.
[15] W. Cassing, W. Ehehalt, and C. M. Ko, Phys. Lett. B363 (1995) 35.
[16] W. Cassing, W. Ehehalt, and I. Kralik, Phys. Lett. B377 (1996) 5.
[17] D. K. Srivastava, B. Sinha, and C. Gale, Phys. Rev. C53 (1996) R567.
[18] G. Chanfray, R. Rapp, and J. Wambach, Phys. Rev. Lett. 76 (1996) 368.
[19] R. Rapp, G. Chanfray, and J. Wambach, Nucl. Phys. A, in press
[20] V. Koch and C. Song, Phys. Rev. C 54 (1996) 1903.
[21] J.M. Steele, H. Yamagishi, and I. Zahed, Phys. Lett. B 384 (1996) 255.
[22] J.M. Steele, H. Yamagishi, and I. Zahed, hep-ph/9704414.
[23] C. M. Hung and E. Shuryak, hep-ph/9608299.
[24] J. Sollfrank, P. Huovinen, M. Kataja, P.V. Ruuskanen, M. Prakash, and R. Venugopalan, Phys. Rev. C55 (1997) 392.
[25] R. Baier, M. Dirks, and K. Redlich, hep-ph/9612448.
[26] G.E. Brown and M. Rho, Phys. Rev. Lett. 66 (1991) 2720.
[27] B. Friman, Nucl. Phys. A610 (1996) 358c.
[28] F. Klingl and W. Weise, Nucl. Phys. A606 (1996) 329.
[29] J. Kapusta, D. Kharzeev, and L. McLerran, Phys. Rev. D 53 (1996) 5028.
[30] Z. Huang and X.-N. Wang, Phys. Rev. D 53 (1996) 5041.
[31] R. Santo *et al.,* Nucl. Phys. A566 (1994) 61c
[32] T.C. Awes *et al.,* Nucl. Phys. A590 (1995) 81c.
[33] R. Albrecht *et al.,* Phys. Rev. Lett. 76 (1996) 3506.
[34] R. Baur *et al.,* Z. Phys. C 71 (1996) 577.
[35] E.V. Shuryak and L. Xiong, Phys. Lett. B 333 (1994) 316.
[36] D. K. Srivastava and B. Sinha, Phys. Rev. Lett. 73 (1994) 2421.
[37] N. Arbex, U. Ornik, M. Plümer, A. Timmermann, and R.M. Weiner, Phys. Lett. B 345 (1995) 307.
[38] A. Dumitru, U. Katscher, J.A. Maruhn, H. Stöcker, W. Greiner, and D.H. Rischke, Phys. Rev. C 51 (1995) 2166.
[39] J.J. Neumann, D. Seibert, and G. Fai, Phys. Rev. C 51 (1995) 1460.
[40] J. Cleymans, K. Redlich, and D.K. Srivastava, Phys. Rev. C 55 (1997) 1431.
[41] T. Hirano, S. Muroya, and M. Namiki, hep-ph/9612234.
[42] E.L. Bratkovskaya and W. Cassing, Nucl. Phys. A, in press.
[43] C. M. Ko, Q. Li, and R. Wang, Phys. Rev. Lett. 59 (1987) 1084; C. M. Ko and Q. Li, Phys. Rev. C37 (1988) 2270.
[44] C.M. Ko and G.Q. Li, Jour. Phys. G22 (1996) 1673.
[45] C.M. Ko, V. Koch, and G.Q. Li, Ann. Rev. Nucl. Part. Sci. 1997, to be published.
[46] B. D. Serot and J. D. Walecka, Adv. Nucl. Phys. 16 (1986) 1.
[47] H. Sorge, H. Stöcker, and W. Greiner, Ann. Phys. 192 (1989) 266.
[48] B.J. VerWest and R.A. Arndt, Phys. Rev. C 25 (1982) 1979.
[49] Gy. Wolf, W. Cassing, and U. Mosel, Nucl. Phys. A 552 (1993) 549.
[50] P. Danielewicz and G.F. Bertsch, Nucl. Phys. A533 (1991) 712.
[51] T. Hatsuda and S. H. Lee, Phys. Rev. C46 (1992) R34.
[52] K. Saito and A. W. Thomas, Phys. Rev. C51 (1995) 2757.
[53] R.J. Furnstahl, H.-B. Tang, and B.D. Serot, Phys. Rev. C 52 (1995) 1368.
[54] G.Q. Li, G.E. Brown, C.-H. Lee, and C.M. Ko, to be published.
[55] R. Albrecht *et al.,* Z. Phys. C 55 (1992) 539.
[56] R. Santo *et al.,* Nucl. Phys. A566 (1994) 61c.
[57] R. Bauer *et al.,* Nucl. Phys. A566 (1994) 87c.
[58] Particle Data Group, Phys. Rev. D 54 (1996) 1.
[59] P. Singer, Phys. Rev. 130 (1963) 2441.
[60] Ö. Kaymakcalan, S. Rajeev, and J. Schechter, Phys. Rev. D 30 (1984) 594.

[61] M. Zielinski, Phys. Rev. Lett. 52 (1984) 1195.
[62] L. Xiong, E. Shuryak, and G.E. Brown, Phys. Rev. D 46 (1992) 3798.
[63] J.L. Rosner, Phys. Rev. D 23 (1981) 1127.
[64] J. Kapusta, P. Lichard, and D. Seibert, Phys. Rev. D 44 (1991) 2774.
[65] C. Song, Phys. Rev. C 47 (1993) 2861.
[66] M. Bando, T. Kugo, and K. Yamawaki, Phys. Rep. 164 (1988) 217.
[67] G.E. Brown, M.A. Halasz, G.Q. Li, and J.V. Steele, work in progress.

Figure Captions

Fig. 1: Pseudorapity distribution of charged hadrons (upper window) and pion transverse momentum spectra (lower window) in central S+Au collisions at 200 AGeV.

Fig. 2: Decay width for $\rho \to \pi\pi\gamma$ as a function of rho meson mass. The open circle is experimental data for ρ^0.

Fig. 3: Radiative decay widths of ω (upper window) and a_1 (lower window) mesons as a function of their masses. The open circles are experimental data.

Fig. 4: Cross sections for $\pi\pi \to \rho\gamma$ from Ref. [64], for three different masses.

Fig. 5: Cross sections for $\pi\rho \to \pi\gamma$ from Ref. [64], for three different masses.

Fig. 6: Backgroud single photon spectra from π^0 and η decays in central S+Au collisions.

Fig. 7: thermal single photon spectra from ρ, ω, η' and a_1 decays (left window), from N^*, Δ^* and Σ^0 decays (middle window), and from $\pi\pi$ and $\pi\rho$ scattering (right window) in central S+Au collisions.

Fig. 8: thermal single photon spectra meson decay (dotted line), baryon decay (short-dashed), and two-body scattering (long-dashed) in central S+Au collisions. The solid circles give the upper bound from the WA80 collaboration [33].

Fig. 9: Same as Fig 7, the results with in-medium meson masses.

Fig. 10: Same as Fig. 8, the results with in-medium meson masses.

Fig. 11: The ratio of total photon spectra to the backgroud photon spectra in central S+Au collisions. The solid and dashed histograms are the results with in-medium and free meson masses, respectively. The solid circles are the experimental data from the WA80 collaboration [33].

Fig. 12: Comparison of our results with those of Ref. [24] (dotted line) and Ref. [36] (long-dashed line).

Fig. 13: Comparison of our results with those of Ref. [22]. Upper window: pions only, lower window: pions and baryons.

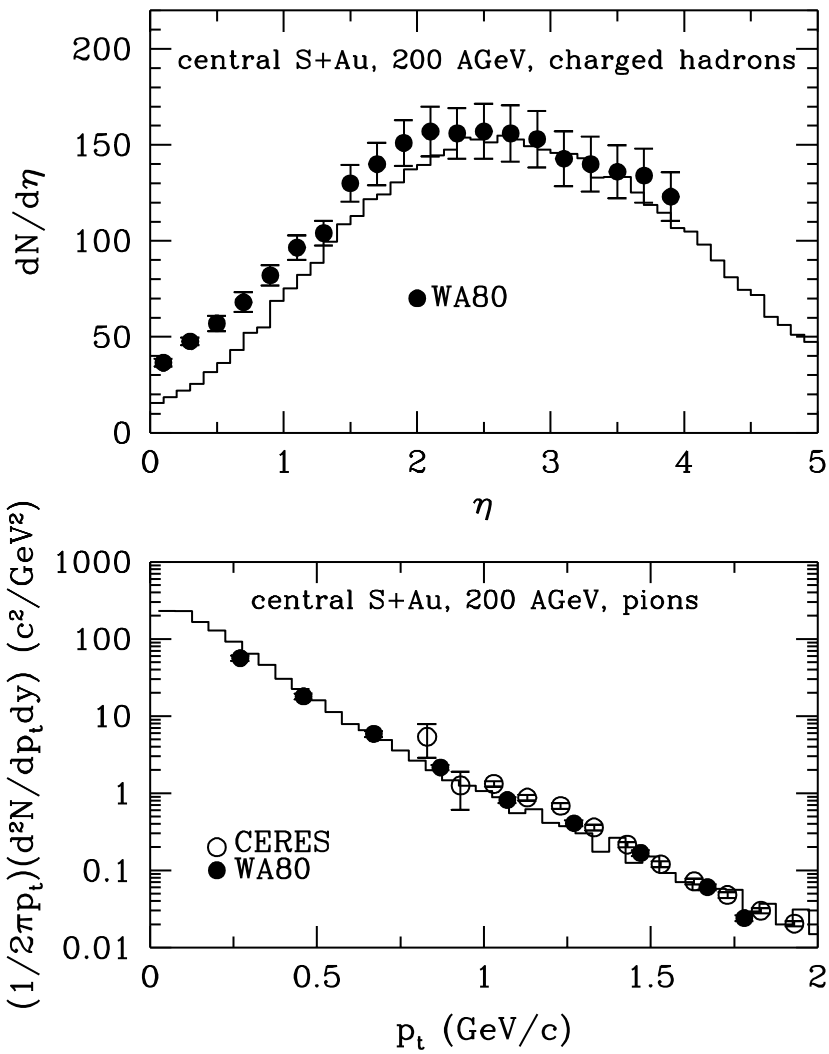
central S+Au, 200 AGeV, charged hadrons
WA80
dN/dη
η
central S+Au, 200 AGeV, pions
CERES
WA80
(1/2πp_t)(d²N/dp_t dy) (c²/GeV²)
p_t (GeV/c)

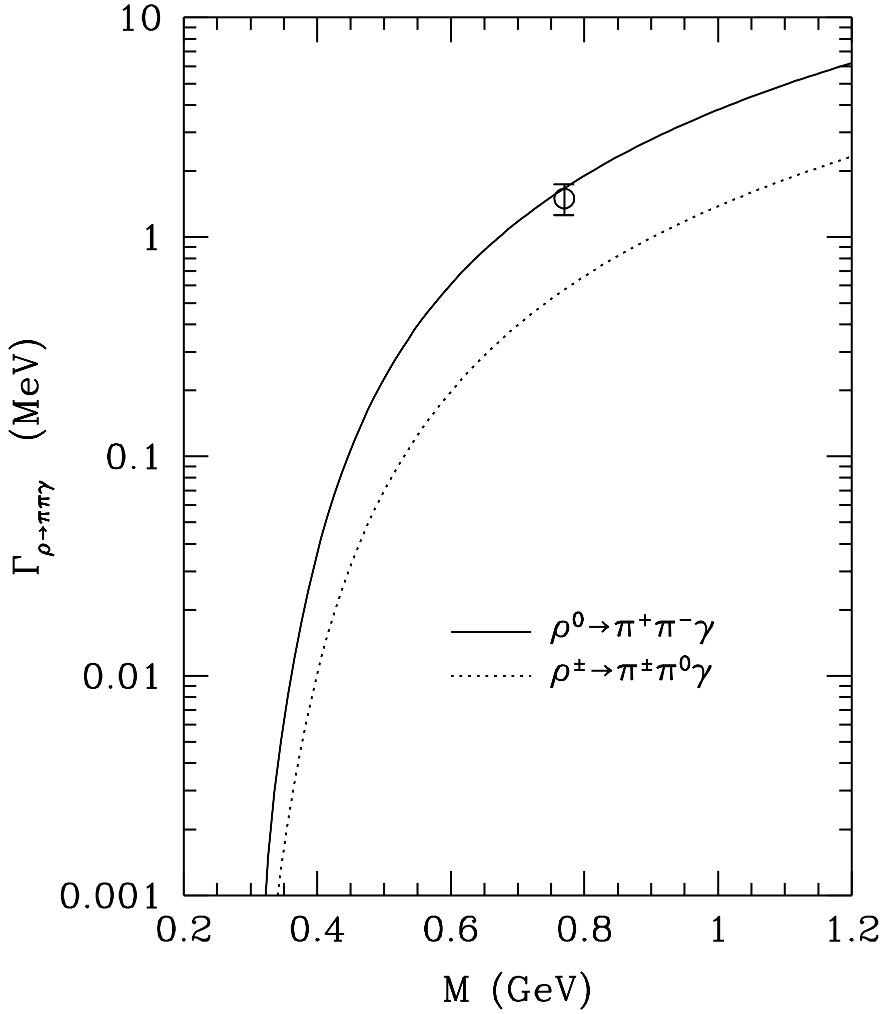
10
1
0.1
0.01
0.001
0.2
0.4
0.6
0.8
1
1.2
M (GeV)
$\Gamma_{\rho\to\pi\pi\gamma}$ (MeV)
$\rho^0\to\pi^+\pi^-\gamma$
$\rho^\pm\to\pi^\pm\pi^0\gamma$

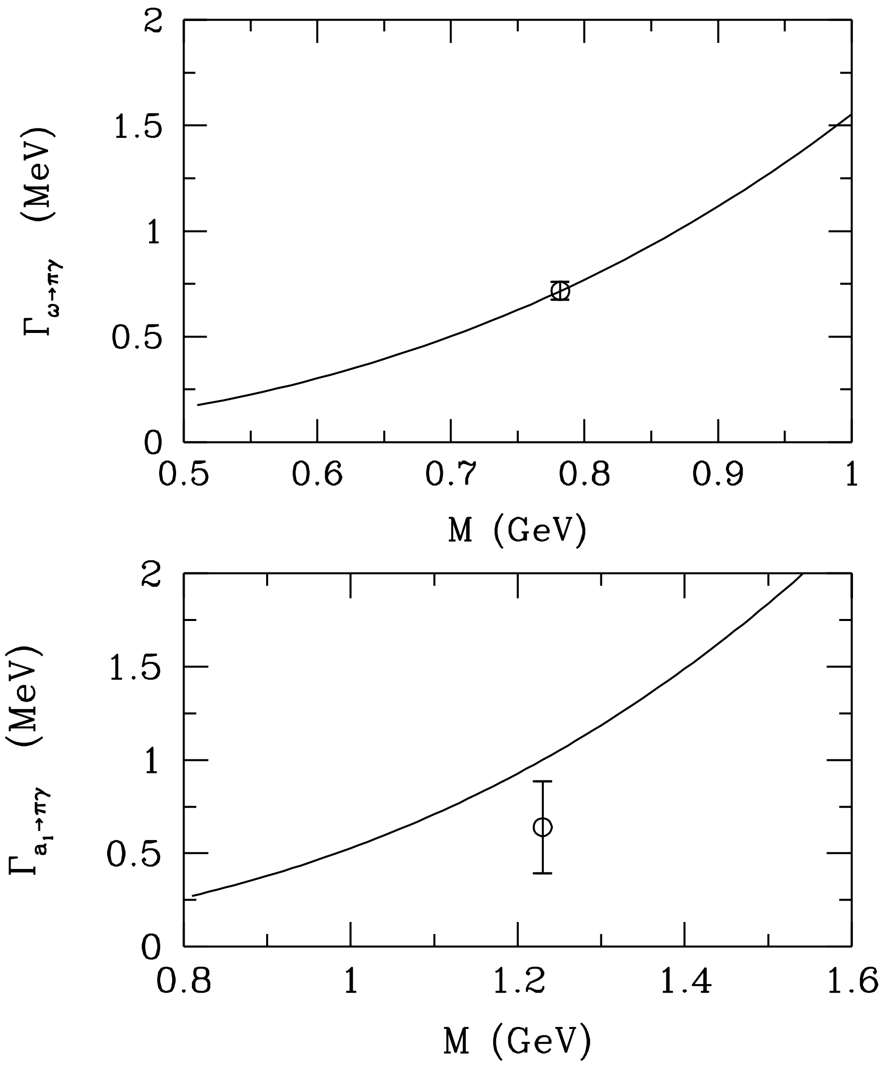

$\Gamma_{\omega\to\pi\gamma}$ (MeV)
M (GeV)
$\Gamma_{a_1\to\pi\gamma}$ (MeV)
M (GeV)

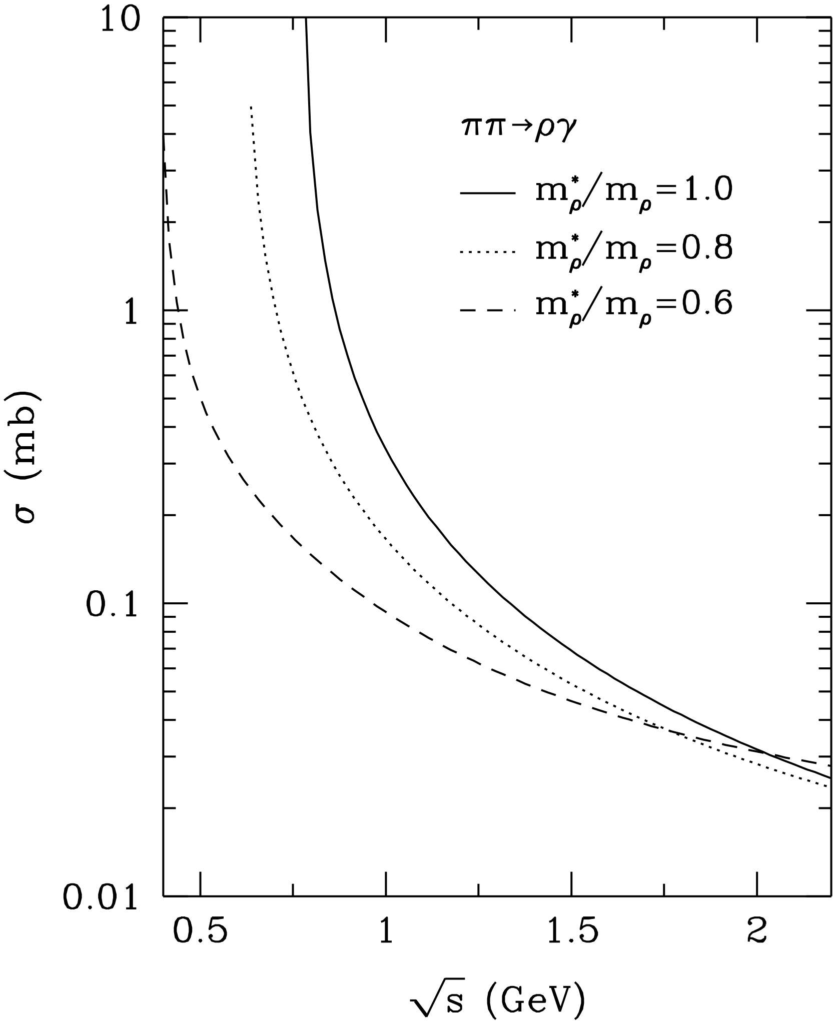
10
1
0.1
0.01
0.5
1
1.5
2
σ (mb)
$\sqrt{s}$ (GeV)
$\pi\pi \to \rho\gamma$
$m_\rho^*/m_\rho=1.0$
$m_\rho^*/m_\rho=0.8$
$m_\rho^*/m_\rho=0.6$

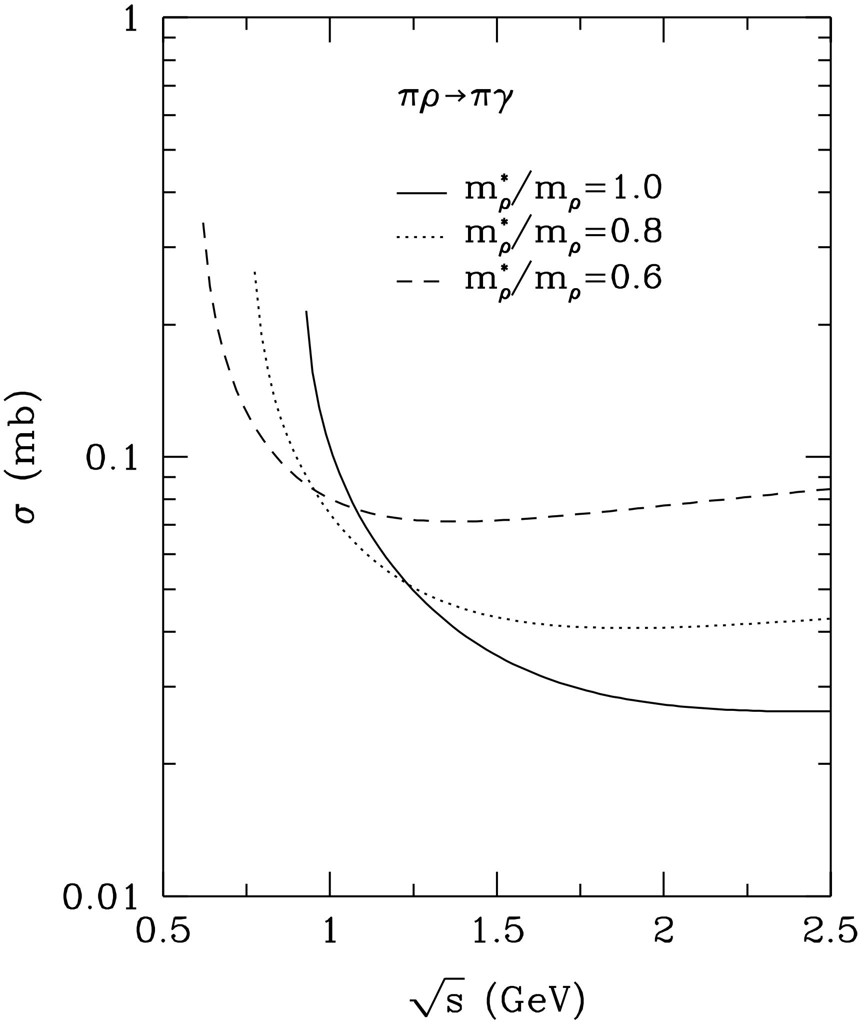

$\pi\rho \to \pi\gamma$
$m_\rho^*/m_\rho=1.0$
$m_\rho^*/m_\rho=0.8$
$m_\rho^*/m_\rho=0.6$
σ (mb)
$\sqrt{s}$ (GeV)
1
0.1
0.01
0.5
1
1.5
2
2.5

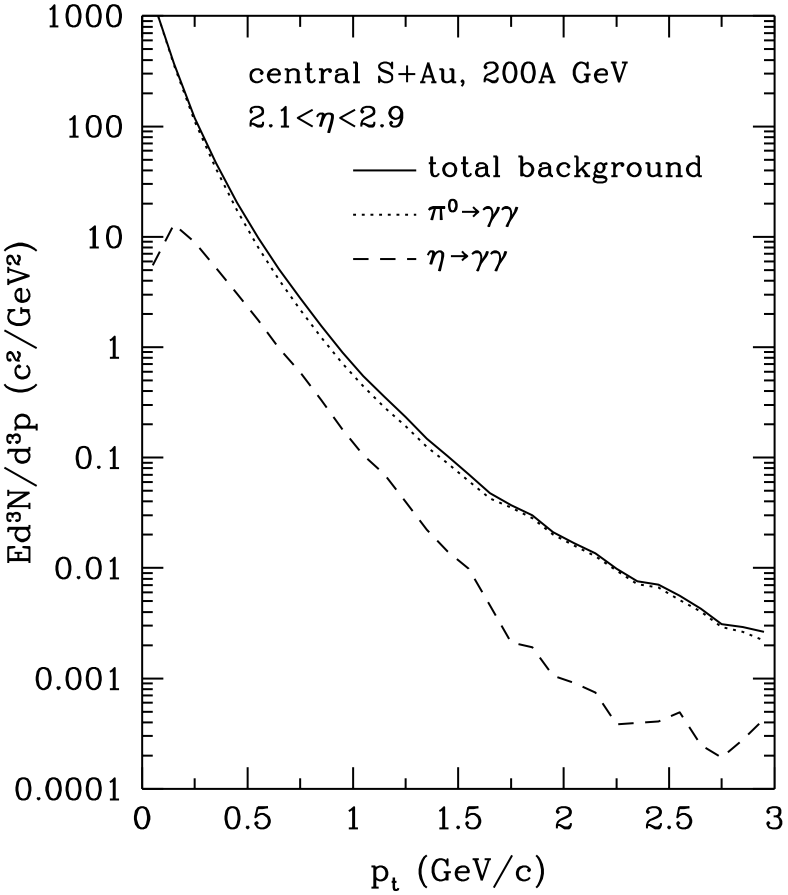

central S+Au, 200A GeV
2.1<η<2.9
total background
π⁰→γγ
η→γγ
Ed³N/d³p (c²/GeV²)
p_t (GeV/c)
1000
100
10
1
0.1
0.01
0.001
0.0001
0
0.5
1
1.5
2
2.5
3

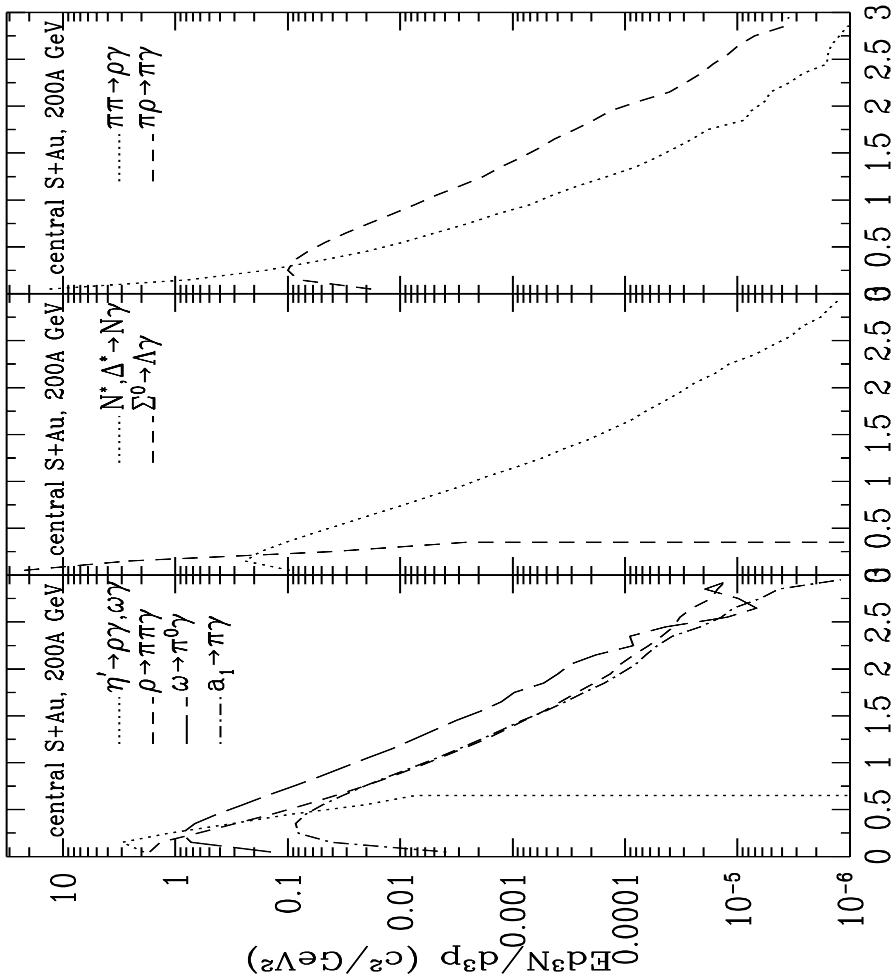

central S+Au, 200A GeV
$\eta' \to \rho\gamma, \omega\gamma$
$\rho \to \pi\pi\gamma$
$\omega \to \pi^0\gamma$
$a_1 \to \pi\gamma$
central S+Au, 200A GeV
$N^*, \Delta^* \to N\gamma$
$\Sigma^0 \to \Lambda\gamma$
central S+Au, 200A GeV
$\pi\pi \to \rho\gamma$
$\pi\rho \to \pi\gamma$
p_t (GeV/c)
p_t (GeV/c)
p_t (GeV/c)
Ed^3N/d^3p (c^2/GeV^2)

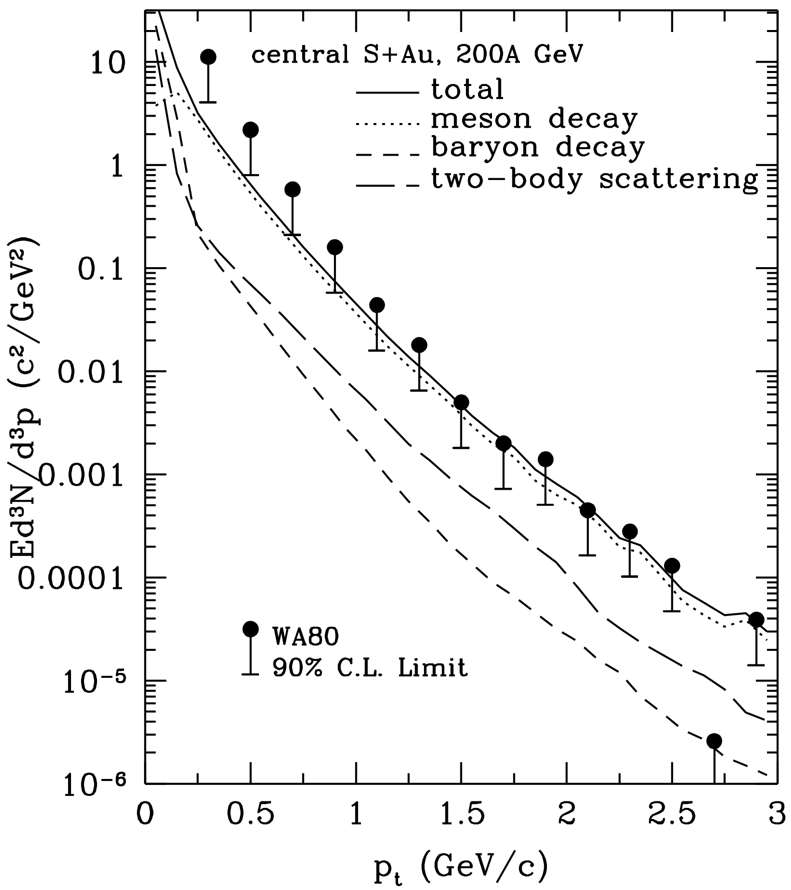
central S+Au, 200A GeV
total
meson decay
baryon decay
two−body scattering
WA80
90% C.L. Limit
Ed³N/d³p (c²/GeV²)
10
1
0.1
0.01
0.001
0.0001
10⁻⁵
10⁻⁶
0
0.5
1
1.5
2
2.5
3
p_t (GeV/c)

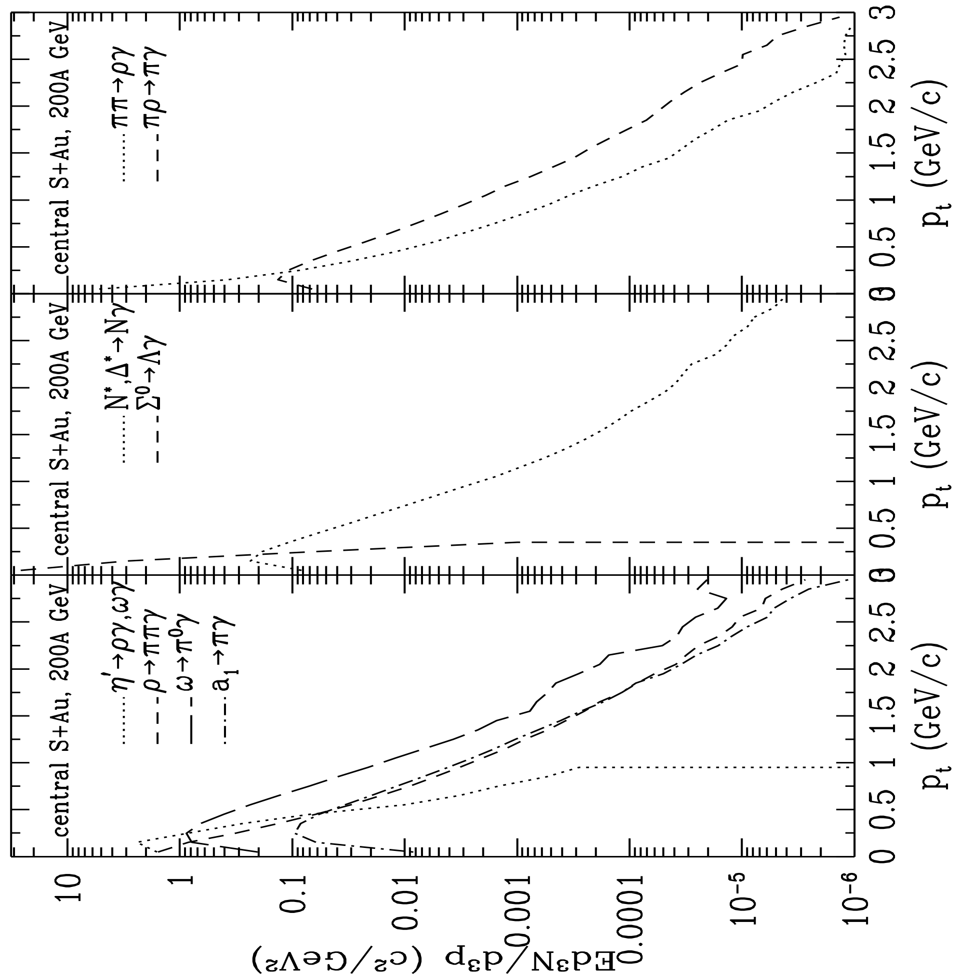
central S+Au, 200A GeV
η′→ργ,ωγ
ρ→ππγ
ω→π⁰γ
a₁→πγ
N*,Δ*→Nγ
Σ⁰→Λγ
ππ→ργ
πρ→πγ
p_t (GeV/c)
Ed3N/d3p (c²/GeV²)

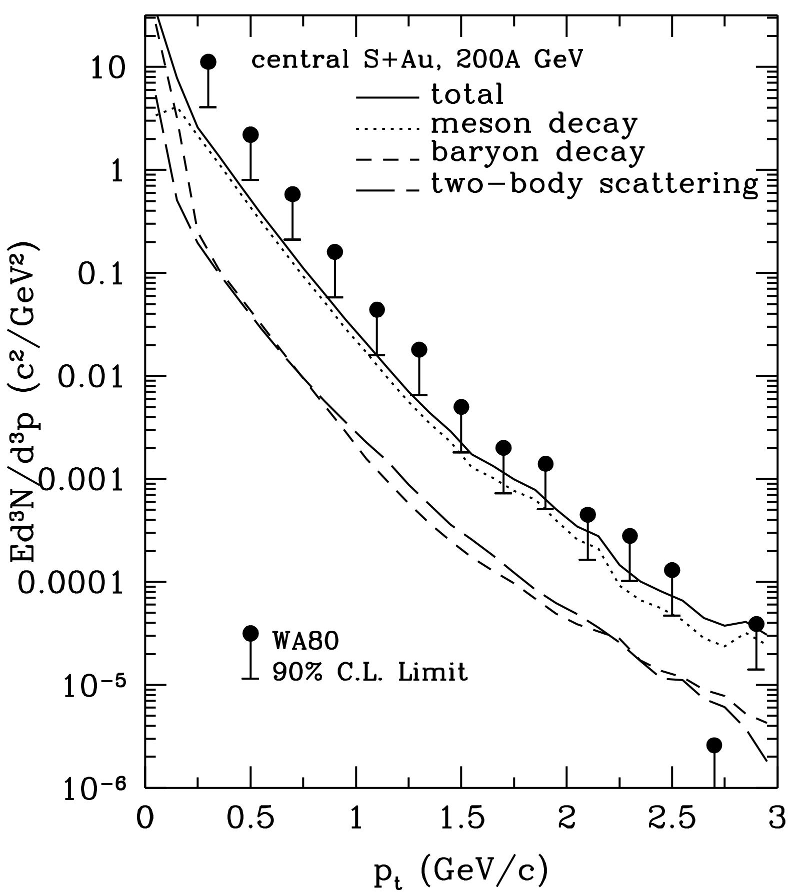

central S+Au, 200A GeV
total
meson decay
baryon decay
two−body scattering
WA80
90% C.L. Limit
10
1
0.1
0.01
0.001
0.0001
10⁻⁵
10⁻⁶
0
0.5
1
1.5
2
2.5
3
Ed³N/d³p (c²/GeV²)
p_t (GeV/c)

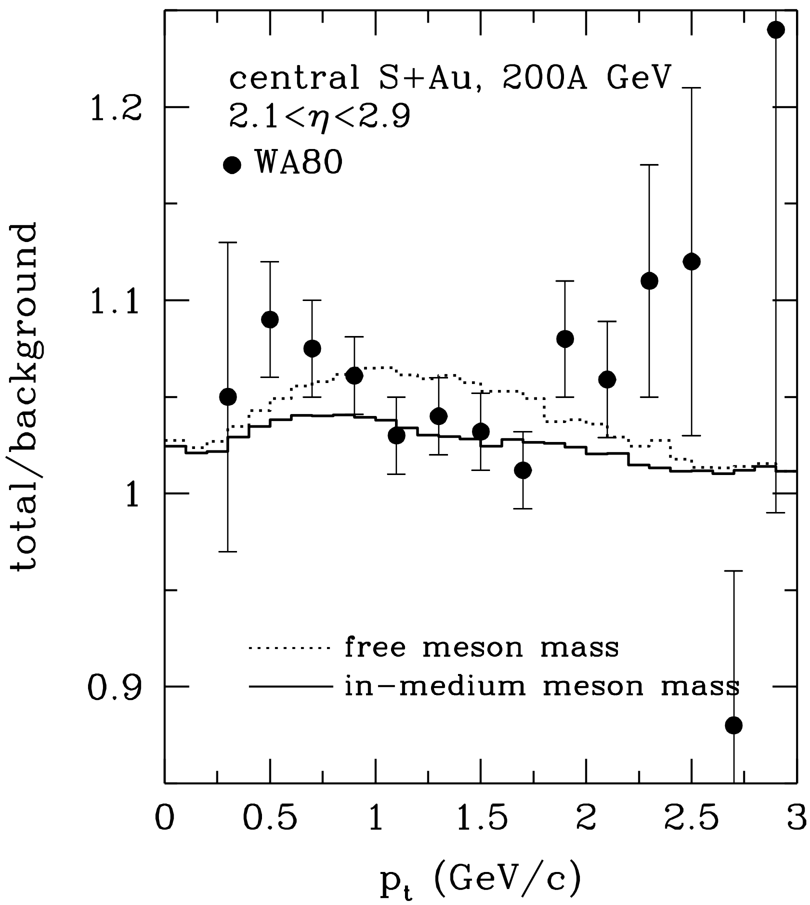
central S+Au, 200A GeV
2.1<η<2.9
WA80
free meson mass
in−medium meson mass
total/background
1.2
1.1
1
0.9
0
0.5
1
1.5
2
2.5
3
p_t (GeV/c)

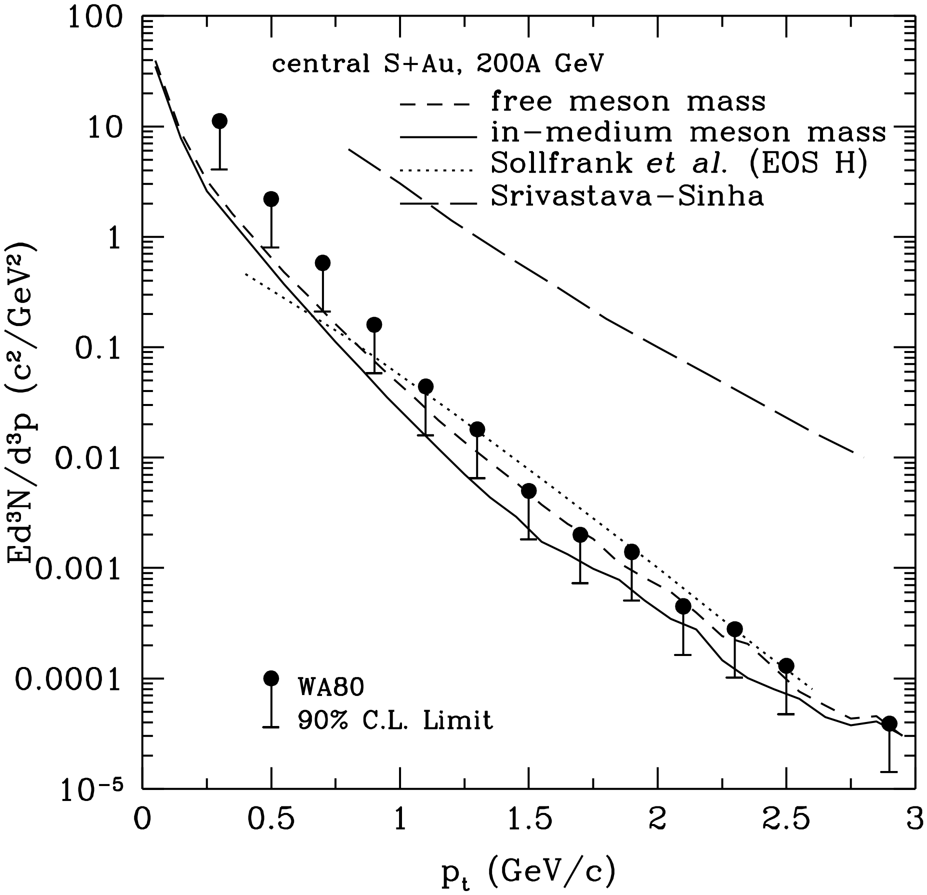

central S+Au, 200A GeV
free meson mass
in−medium meson mass
Sollfrank *et al.* (EOS H)
Srivastava−Sinha
WA80
90% C.L. Limit
Ed³N/d³p (c²/GeV²)
p_t (GeV/c)
100
10
1
0.1
0.01
0.001
0.0001
10⁻⁵
0
0.5
1
1.5
2
2.5
3

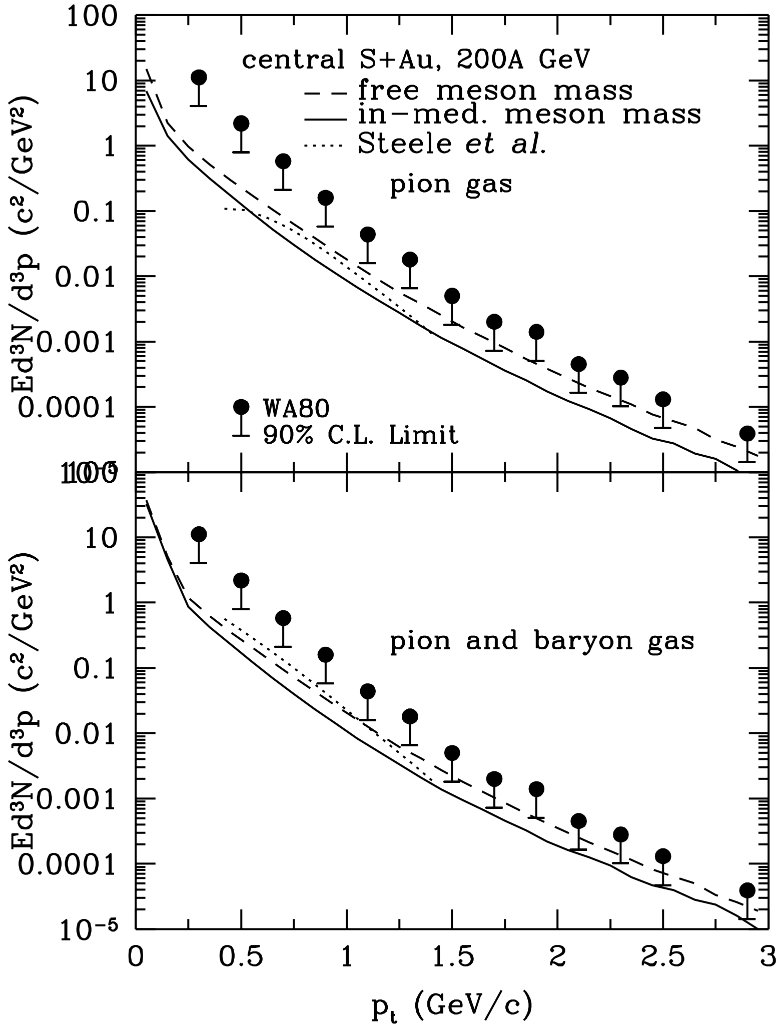

central S+Au, 200A GeV
free meson mass
in−med. meson mass
Steele et al.
pion gas
WA80
90% C.L. Limit
pion and baryon gas
Ed³N/d³p (c²/GeV²)
p_t (GeV/c)